

Charged Boson Stars and Black Holes

Burkhard Kleihaus, Jutta Kunz

Institut für Physik, Universität Oldenburg, Postfach 2503
D-26111 Oldenburg, Germany

Claus Lämmerzahl, Meike List

ZARM, Universität Bremen, Am Fallturm
D-28359 Bremen, Germany

February 12, 2022

Abstract

We consider boson stars and black holes in scalar electrodynamics with a V-shaped scalar potential. The boson stars come in two types, having either ball-like or shell-like charge density. We analyze the properties of these solutions and determine their domains of existence. When mass and charge become equal, the space-times develop a throat. The shell-like solutions need not be globally regular, but may possess a horizon. The space-times then consist of a Schwarzschild-type black hole in the interior, surrounded by a shell of charged matter, and thus a Reissner-Nordström-type space-time in the exterior. These solutions violate black hole uniqueness. The mass of the black hole solutions is related to the mass of the regular shell-like solutions by a mass formula of the type first obtained within the isolated horizon framework.

1 Introduction

Q -balls represent stationary localized solutions of a complex scalar field theory with a suitable self-interaction in flat space [1, 2]. The global phase invariance of the scalar field theory is associated with a conserved charge Q [1], which represents the electromagnetic charge, once the theory is promoted to a gauge theory.

The simplest type of Q -balls is spherically symmetric. These possess a finite mass and charge, but carry no angular momentum. Considering their mass as a function of their charge, there are two branches of Q -balls, merging and ending at a cusp, where mass and charge assume their minimal values [1].

Recently, a new type of scalar potential for Q -balls was considered, leading to the signum-Gordan equation for the scalar field [3, 4]. This potential gives rise to spatially compact Q -balls, where the scalar field vanishes identically outside a critical radius r_o [3]. When coupled to electromagnetism, a new type of solution appears, Q -shells [4]. In Q -shells the scalar field vanishes identically both inside a critical radius r_i and outside a critical radius r_o , thus forming a finite shell $r_i < r < r_o$ of charged matter.

When gravity is coupled to Q -balls, boson stars arise, representing globally regular self-gravitating solutions [5, 6, 7, 8]. The presence of gravity has a crucial influence on the domain of existence of the classical solutions. Instead of only two branches of solutions joint at a single cusp, the boson stars exhibit an intricate cusp structure, where mass and charge oscillate endlessly. For

black holes with scalar fields, on the other hand, a number of theorems exist, which exclude their existence under a large variety of conditions [9, 10, 11].

Here we consider the effect of gravity on the Q -balls and Q -shells of the signum-Gordon model coupled to a Maxwell field. We construct these charged boson stars and gravitating Q -shells and analyze their properties and their domains of existence. We observe that at certain critical values of the mass and charge, the space-times form a throat at the (outer) radius r_o , rendering the respective exterior space-time an exterior extremal Reissner-Nordström space-time.

Moreover, we show that in this model the black hole theorems can be elluded, that forbid black holes with scalar hair. Indeed, the gravitating Q -shells can be endowed with a horizon r_H in the interior region $0 < r_H < r_i$, where the scalar field vanishes and the gauge potential is constant. This Schwarzschild-type black hole in the interior is surrounded by a shell of charged matter, $r_i < r < r_o$, leading to an exterior space-time $r_o < r < \infty$ of Reissner-Nordström type. We analyze the global and horizon properties of these black holes within Q -shells, and present a mass relation. When a throat develops at the outer radius r_o , which renders the respective exterior space-time an exterior extremal Reissner-Nordström space-time, the temperature of the horizon r_H tends to zero.

In section 2 we recall the action and ansätze for the fields. We present the gravitating Q -balls and Q -shells in section 3 and 4, respectively, and the black holes within Q -shells in section 5. We end with a conclusion and an outlook.

2 Action

We consider the action of a self-interacting complex scalar field Φ coupled to a U(1) gauge field and to Einstein gravity

$$S = \int \left[\frac{R}{16\pi G} - \frac{1}{4} F^{\mu\nu} F_{\mu\nu} - (D_\mu \Phi)^* (D^\mu \Phi) - U(|\Phi|) \right] \sqrt{-g} d^4x, \quad (1)$$

with field strength tensor

$$F_{\mu\nu} = \partial_\mu A_\nu - \partial_\nu A_\mu, \quad (2)$$

covariant derivative

$$D_\mu \Phi = \partial_\mu \Phi + ie A_\mu \Phi, \quad (3)$$

curvature scalar R , Newton's constant G , gauge coupling constant e , and the asterisk denotes complex conjugation. The scalar potential U is chosen as

$$U(|\Phi|) = \lambda |\Phi|^4. \quad (4)$$

Variation of the action with respect to the metric and the matter fields leads, respectively, to the Einstein equations

$$G_{\mu\nu} = R_{\mu\nu} - \frac{1}{2} g_{\mu\nu} R = 8\pi G T_{\mu\nu} \quad (5)$$

with stress-energy tensor

$$\begin{aligned} T_{\mu\nu} &= g_{\mu\nu} L_M - 2 \frac{\partial L_M}{\partial g^{\mu\nu}} = (F_{\mu\alpha} F_{\nu\beta} g^{\alpha\beta} - \frac{1}{4} g_{\mu\nu} F_{\alpha\beta} F^{\alpha\beta}) \\ &- \frac{1}{2} g_{\mu\nu} ((D_\alpha \Phi)^* (D_\beta \Phi) + (D_\beta \Phi)^* (D_\alpha \Phi)) g^{\alpha\beta} + (D_\mu \Phi)^* (D_\nu \Phi) + (D_\nu \Phi)^* (D_\mu \Phi) \\ &- \lambda g_{\mu\nu} |\Phi|^4, \end{aligned} \quad (6)$$

and the matter field equations,

$$\partial_\mu (\sqrt{-g} F^{\mu\nu}) = \sqrt{-g} e \Phi^* D^\nu \Phi \quad (7)$$

$$D_\mu D^\mu \Phi = -\frac{\lambda}{2} \frac{\Phi}{|\Phi|}. \quad (8)$$

To construct static spherically symmetric solutions we employ Schwarzschild-like coordinates and adopt the spherically symmetric metric

$$ds^2 = g_{\mu\nu} dx^\mu dx^\nu = -A^2 N dt^2 + N^{-1} dr^2 + r^2 (d\theta^2 + \sin^2 \theta d\phi^2), \quad (9)$$

with

$$N = 1 - \frac{2m(r)}{r}. \quad (10)$$

For solutions with vanishing magnetic field the Ansatz for the matter fields has the form

$$\Phi = \phi(r) e^{i\omega t}, \quad (11)$$

$$A_\mu dx^\mu = A_0(r) dt. \quad (12)$$

For notational simplicity, we introduce new coupling constants [4]

$$\alpha^2 = a = 4\pi G \frac{\beta^{1/3}}{e^2}, \quad \beta = \frac{\lambda e}{\sqrt{2}}, \quad (13)$$

and redefine the matter field functions,

$$h(r) = \sqrt{2} e \phi(r), \quad b(r) = \omega + e A_0(r). \quad (14)$$

The latter corresponds to performing a gauge transformation to make the scalar field real and absorbing the frequency ω of the scalar field into the gauge transformed vector potential. Note, that the parameter β can be removed by rescaling and will therefore be set to one [4]. Thus the only parameter left is the gravitational coupling α .

Let us now specify the boundary conditions for the metric and matter functions. For the metric function A we adopt

$$A(r_o) = 1, \quad (15)$$

where r_o is the outer radius, thus fixing the time coordinate. For the mass function $m(r)$ we require for globally regular ball-like boson star solutions

$$m(0) = 0, \quad (16)$$

for globally regular shell-like solutions

$$m(r_i) = 0, \quad (17)$$

where r_i is the inner radius of the shell, and for black hole solutions

$$m(r_H) = \frac{r_H}{2} \quad (18)$$

where $r_H < r_i$ denotes the horizon.

To be able to specify more than four boundary conditions for the matter functions we introduce one or more auxiliary variables. For globally regular boson star solutions we require at the origin and at the outer radius r_o the conditions

$$b'(0) = 0, \quad h'(0) = 0, \quad h(r_o) = 0, \quad h'(r_o) = 0, \quad (19)$$

where the prime denotes differentiation with respect to r . In order to choose also the value of $b(0)$ as a boundary condition, we make the outer radius r_o an auxiliary (constant) variable, and thus add the differential equation $r_o' = 0$, without imposing a boundary condition.

For globally regular shell solutions as well as for black holes we require at the inner radius r_i and at the outer radius r_o the conditions

$$b'(r_i) = 0, \quad h(r_i) = 0, \quad h'(r_i) = 0, \quad h(r_o) = 0, \quad h'(r_o) = 0. \quad (20)$$

In order to choose also the value of $b(r_i)$ as a boundary condition, we now also make the ratio of inner and outer radius r_i/r_o an auxiliary (constant) variable. Alternatively to demanding a certain value for $b(r_i)$, we may also specify the value of the electric charge Q .

The charge Q of the solutions is associated with the conserved current

$$j^\mu = -i(\Phi^* D^\mu \Phi - \Phi D^\mu \Phi^*) , \quad j^\mu_{;\mu} = 0 , \quad (21)$$

i.e., the charge is obtained as the spatial integral

$$Q = -i \int j^0 \sqrt{-g} dr d\theta d\varphi. \quad (22)$$

The mass M of the stationary asymptotically flat space-times is obtained from the corresponding Komar expression. For globally regular space-times like boson stars and shells of boson matter the mass is given by

$$M = \frac{1}{4\pi G} \int_{\Sigma} R_{\mu\nu} n^\mu \xi^\nu dV, \quad (23)$$

where Σ denotes an asymptotically flat spacelike hypersurface, n^μ is normal to Σ with $n_\mu n^\mu = -1$, dV is the natural volume element on Σ , and ξ denotes an asymptotically timelike Killing vector field [12]. Replacing the Ricci tensor via the Einstein equations by the stress-energy tensor yields

$$M = 2 \int_{\Sigma} \left(T_{\mu\nu} - \frac{1}{2} g_{\mu\nu} T_\gamma{}^\gamma \right) n^\mu \xi^\nu dV. \quad (24)$$

For black hole space-times the corresponding Komar expression is given by

$$M = M_H + 2 \int_{\Sigma} \left(T_{\mu\nu} - \frac{1}{2} g_{\mu\nu} T_\gamma{}^\gamma \right) n^\mu \xi^\nu dV, \quad (25)$$

where M_H is the horizon mass of the black hole. The mass of all (gravitating) solutions can be directly obtained from the asymptotic form of their metric. In the units employed, we find

$$M = \frac{1}{\alpha^2} \lim_{r \rightarrow \infty} m(r). \quad (26)$$

3 Boson Stars

We first address the set of globally regular ball-like boson star solutions, obtained by coupling the Q -ball solutions [4] to gravity. We illustrate the physical properties of these solutions in Fig. 1.

Fig. 1(a) represents the phase diagram for the boson star solutions. Here the sets of solutions for a sequence of values of the gravitational coupling α are exhibited in terms of the values of the matter field functions at the center of the solutions, i.e., the value of the scalar field function $h(0)$ and the value of the gauge field function $b(0)$. The figure consists of four distinct regions, which we have labelled I, Ia, II and IIa. For $\alpha = 0$, the Q -ball solutions form a continuous set, represented by a single curve in the lower part of the figure, denoted as region I. These non-gravitating solutions are bounded by some maximal value of $h(0)$, by some minimal value of $b(0)$, and by the bifurcation point with the shell-like solutions, where $h(0)$ reaches zero.

As the gravitational coupling constant α is increased from zero, the resulting sets of solutions smoothly deform and fill region I. The maximal value of $h(0)$ of these sets of solutions (for each value of α given by a single continuous curve) then increases, the corresponding minimal value of $b(0)$ decreases, and the bifurcation point with the shell-like solutions decreases as well. This decrease of the bifurcation point continues until zero is reached at the critical value of the gravitational coupling constant, $\alpha_{sh} \approx 0.1861$. Beyond α_{sh} no shell-like solutions exist. However, the set of solutions continues to deform smoothly with increasing α .

This smooth evolution continues, until a second critical value of the gravitational coupling constant α is reached, $\alpha_{cr} \approx 0.1989$. Here a bifurcation with a second set of solutions is encountered,

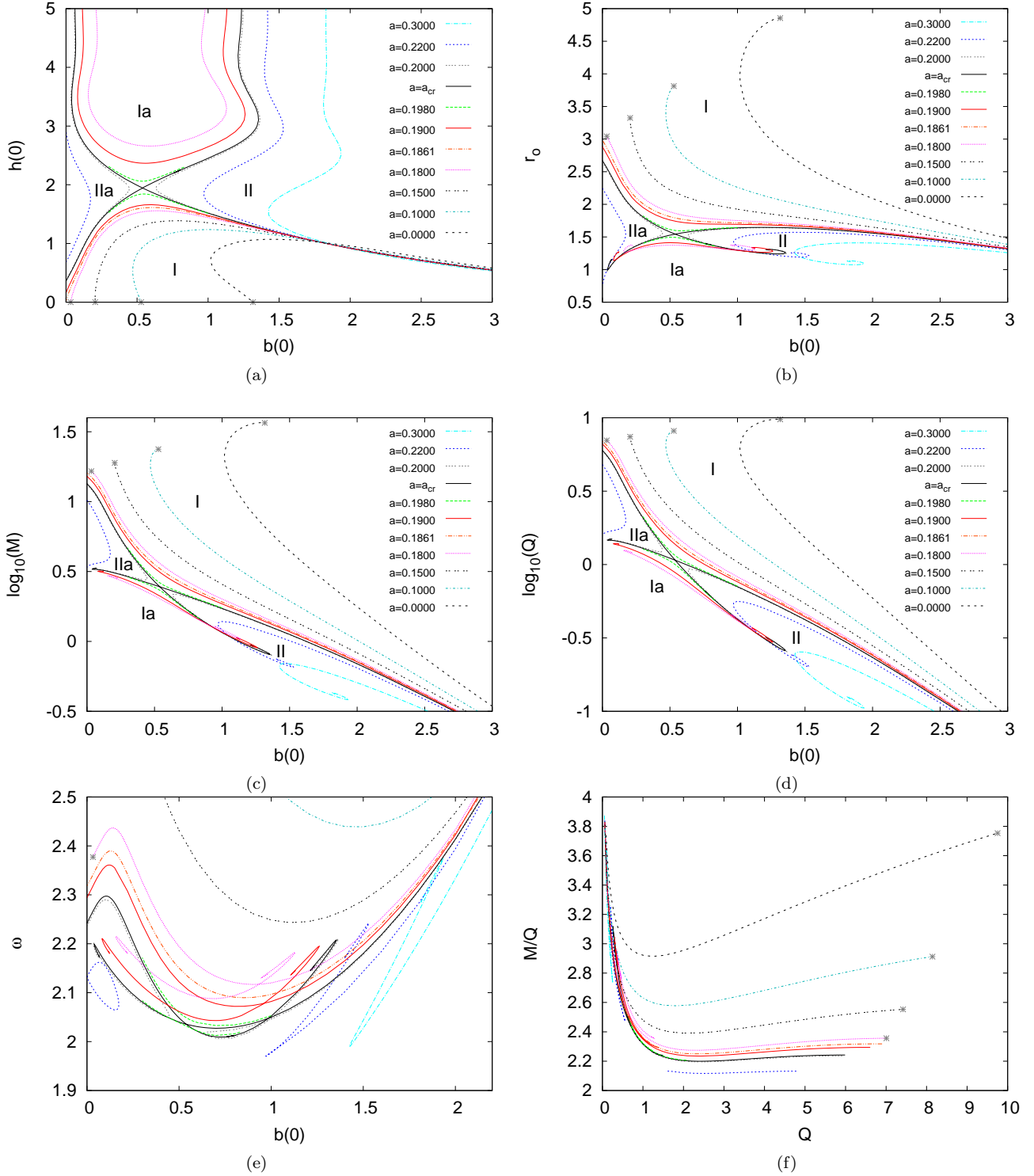


Figure 1: Properties of the boson star solutions shown versus $b(0)$, the value of the gauge field function $b(r)$ at the origin: (a) $h(0)$, the value of the scalar field function $h(r)$ at the origin, forms with $b(0)$ the phase diagram of the solutions; (b) r_o indicates the size of the solutions; (c) and (d) exhibit logarithmically the mass M and the charge Q , respectively; and (e) shows the value $b(\infty)$ of the gauge field function $b(r)$ at infinity (which corresponds to the value of the scalar field frequency ω). In (f) the ratio of mass and charge M/Q is exhibited versus the charge Q . Note that $a = \alpha^2$, and the asterisks mark the transition points from boson stars (Q -balls) to Q -shells.

which constitute the boundary of region Ia. This second type of solutions is present for each finite value of $\alpha \leq \alpha_{cr}$. For this type of solutions $h(0)$ has a minimal value for fixed α , which decreases with increasing α , until at α_{cr} the bifurcation is reached.

At α_{cr} the set I and set Ia solutions touch and bifurcate. For $\alpha > \alpha_{cr}$ they then split into a right and left set of solutions, forming regions II and IIa, respectively. The solutions in region II correspond to the larger values of $b(0)$, while the solutions in region IIa are restricted to the smaller values of $b(0)$. With increasing α , the sets of solutions in region IIa move towards smaller values of $b(0)$, possibly disappearing at some critical value of the gravitational coupling, whereas the sets of solutions in region II move towards larger values of $b(0)$.

Fig. 1(b) shows the outer radius r_o for these sets of solutions, and thus the size of the corresponding boson stars. Clearly, the biggest size for a given $\alpha \leq \alpha_{cr}$ is always reached in region I at the bifurcation point with the shell-like solutions. The oscillations of the gauge field value $b(0)$ with increasing scalar field value $h(0)$ seen in region II in Fig. 1(a) are reflected in the spirals formed by the outer radius r_o in region II in Fig. 1(b). They are also present in regions IIa and Ia, whenever the gauge field value $b(0)$ exhibits oscillations.

The mass M and the charge Q of these sets of boson star solutions are exhibited in Figs. 1(c) and 1(d). Both show a very similar pattern. Again, the biggest mass and charge for a given $\alpha \leq \alpha_{cr}$ are reached in region I at the respective bifurcation point with the shell-like solutions, while the oscillations of $b(0)$ seen in regions Ia, II and IIa lead to spiral patterns for the mass and charge.

The corresponding family of curves for the asymptotic value $b(\infty)$ of the gauge field function $b(r)$ at infinity (which can be identified with the value of the scalar field frequency ω in the gauge, where the gauge field vanishes at infinity) is exhibited in Fig. 1(e). Here the overall pattern is different, but spirals occur as well. Finally, in Fig. 1(f) we exhibit the ratio of mass and charge M/Q versus Q . We observe a linear increase of M/Q with Q for the larger values of Q in regions I and IIa, where the slope decreases with increasing α , making M/Q almost constant for larger values of α (e.g., $\alpha = 0.22$).

While the occurrence of spirals is a typical feature of boson star solutions [1], the present sets of solutions exhibit a for boson stars new phenomenon, namely the formation of throats. As a throat is formed, the minimum of the metric function $N(r)$ tends to zero, and the zero is reached precisely at the outer radius r_o . At the same time the metric function $A(r)$ tends to a step function, that vanishes inside r_o , and assumes the asymptotic value $A(r) = 1$ outside r_o . (In Fig. 2 the functions close to throat formation are exhibited in the case of black holes.)

The space-time for $r \geq r_o$ then corresponds to the exterior space-time of an extremal Reissner-Nordström (RN) black hole. Indeed, there the metric function $N(r)$ can be expressed as

$$N(r) = 1 - \frac{2\alpha^2 M}{r} + \frac{\alpha^2 Q^2}{r^2} = \left(1 - \frac{\alpha Q}{r}\right)^2, \quad (27)$$

i.e., $r_H = r_o = \alpha^2 M = \alpha Q$ for the extremal RN solution (in the units employed). As seen in Fig. 1(f), this relation is precisely satisfied, when $b(0) \rightarrow 0$. Thus a throat is formed, when in a set of solutions the value $b(0)$ of the gauge field function tends to zero. In fact, the function $b(r)$ then tends to zero in the whole region $r < r_o$, and its derivative $b'(r)$ does so as well. However, at r_o the derivative $b'(r)$ jumps to a finite value, necessary for the Coulomb fall-off of a solution with charge Q .

Finally we note, that the sets of boson star solutions with fixed gravitational coupling constant α satisfy a mass relation. This relation is based on the observation, that

$$dM = b(\infty)dQ, \quad (28)$$

shown to hold for the regular solutions in flat space [4]. Since (28) continues to hold for the gravitating solutions, integration yields the mass relation

$$M_2 = M_1 + M_Q = M_1 + \int_{Q_1}^{Q_2} b(\infty)dQ, \quad (29)$$

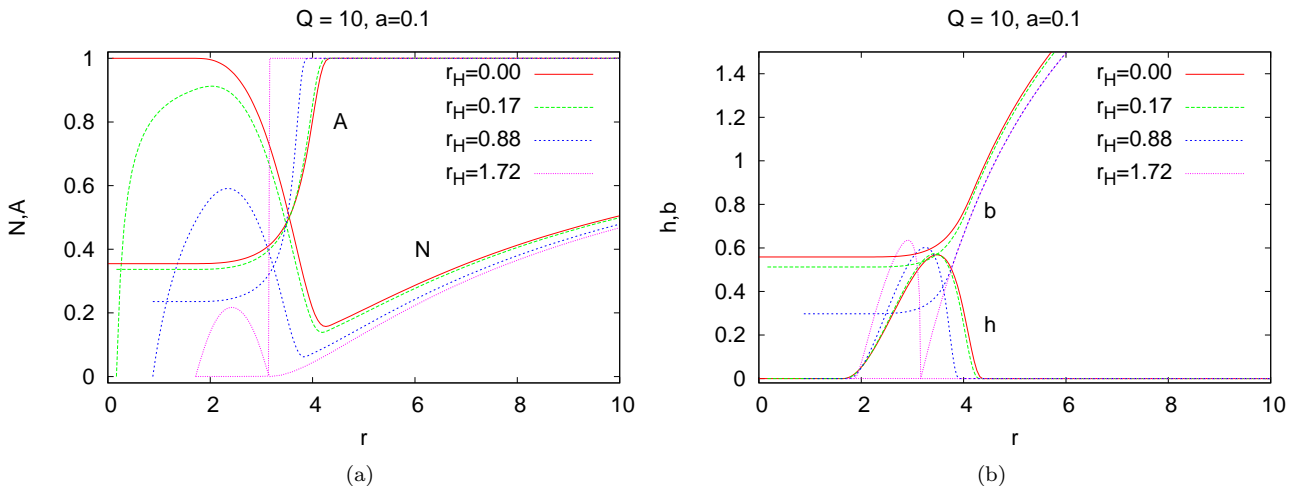


Figure 2: Functions of the gravitating Q -shell solutions shown versus the radial coordinate r for $Q = 10$ and $\alpha^2 = 0.1$: (a) metric functions $A(r)$ and $N(r)$; (b) matter functions $h(r)$ and $b(r)$. Also shown are the corresponding functions for black hole solutions with several horizon radii r_H . The largest r_H is close to the critical value, where the throat is formed.

where the mass M_2 of a regular solution with charge Q_2 is obtained by integrating from any regular solution M_1 with charge Q_1 along the curve of intermediate solutions of the set.

4 Gravitating Q -Shells

Let us next consider the gravitating shell-like solutions. Here the space-time consists of 3 parts. In the inner part $0 \leq r < r_i$ the gauge potential is constant and the scalar field vanishes. Consequently, it is Minkowski-like, with $N(r) = 1$ and $A(r) = \text{const} < 1$. The middle region $r_i < r < r_o$ then represents the shell of charged bosonic matter, while the outer region $r_o < r < \infty$ corresponds to part of a Reissner-Nordström space-time, where the gauge field exhibits the standard Coulomb fall-off, while the scalar field vanishes identically. This behaviour of the functions is demonstrated in Fig. 2 for the shell-like solution with charge $Q = 10$ and gravitational coupling constant $\alpha^2 = 0.1$.

We exhibit in Fig. 3 the properties of shell-like solutions. Fig. 3(a) shows the ratio of the inner radius r_i to the outer radius r_o for these solutions. For a given finite value of the gravitational coupling, the branch of gravitating shells emerges at the corresponding boson star solution and ends, when a throat is formed at the outer radius r_o . As this happens, the value of $b(r_i)$ reaches zero (or equivalently $b(0) \rightarrow 0$, since $b(r)$ is constant in the interior, $0 \leq r \leq r_i$). The exterior space-time $r > r_o$ then corresponds to the exterior of an extremal RN space-time.

Thus in contrast to Q -shells in flat space, which grow rapidly in size, mass and charge as the ratio $r_i/r_o \rightarrow 1$, the growth of gravitating Q -shells is limited by gravity, and the restriction in size, mass and charge is the stronger, the greater the value of the gravitational coupling constant α . This is demonstrated in Figs. 3(b), 3(c) and 3(d), where the outer radius r_o , the mass M and the charge Q are exhibited for a sequence of values of the gravitational coupling constant.

In Fig. 3(c) for comparison also the mass of the corresponding boson star solutions (resp. Q -ball solutions for vanishing gravitational coupling constant) are exhibited. The transitions from the ball-like to the shell-like solutions are indicated in the figure by the small asterisks. With increasing α the sets of shell-like solutions decrease rapidly, until at the critical value α_{sh} (see Fig. 1(a)) they cease to exist.

Fig. 3(d) exhibits the scaled mass $\alpha^2 M$ and the scaled charge αQ for several sets of gravitating

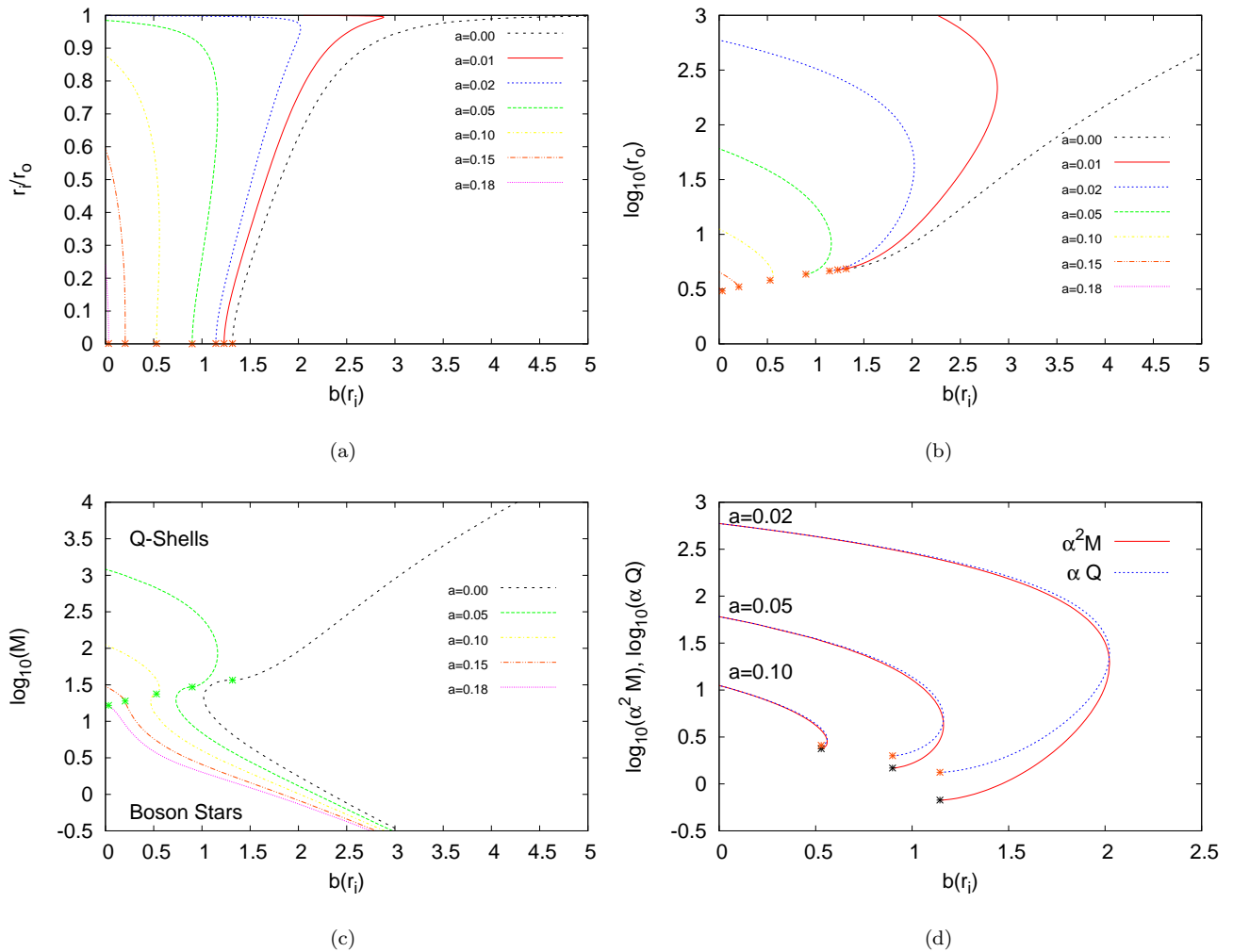


Figure 3: Properties of the gravitating Q -shell solutions shown versus $b(r_i)$, the value of the gauge field function $b(r)$ at the inner shell radius r_i : (a) r_i/r_o , the ratio of inner and outer shell radii; (b) the outer shell radius r_o ; (c) the mass M of shell-like solutions and boson stars (resp. Q -balls for $\alpha = 0$); (d) the scaled mass $\alpha^2 M$ and the scaled charge αQ . Note that $a = \alpha^2$, and the asterisks mark the transition points from boson stars (Q -balls) to Q -shells.

Q -shells. Together with Fig. 3(b) the figure demonstrates, that the condition for extremal RN solutions, $r_o = \alpha^2 M = \alpha Q$, is satisfied for the shell-like solutions, as the throat forms at the outer radius r_o .

Finally we note, that the shell-like solutions satisfy the mass relation (29) as well. Consequently the mass relation holds for any two globally regular solutions of a set with given gravitational coupling constant, thus relating also ball-like and shell-like solutions.

5 Black Holes

Let us finally address black holes in this model. The simplest type of black holes is obtained, when the Minkowski-like inner part of the space-time, $0 \leq r \leq r_i$, of gravitating Q -shell solutions is replaced by the inner part of a curved Schwarzschild-like space-time. The metric in the interior

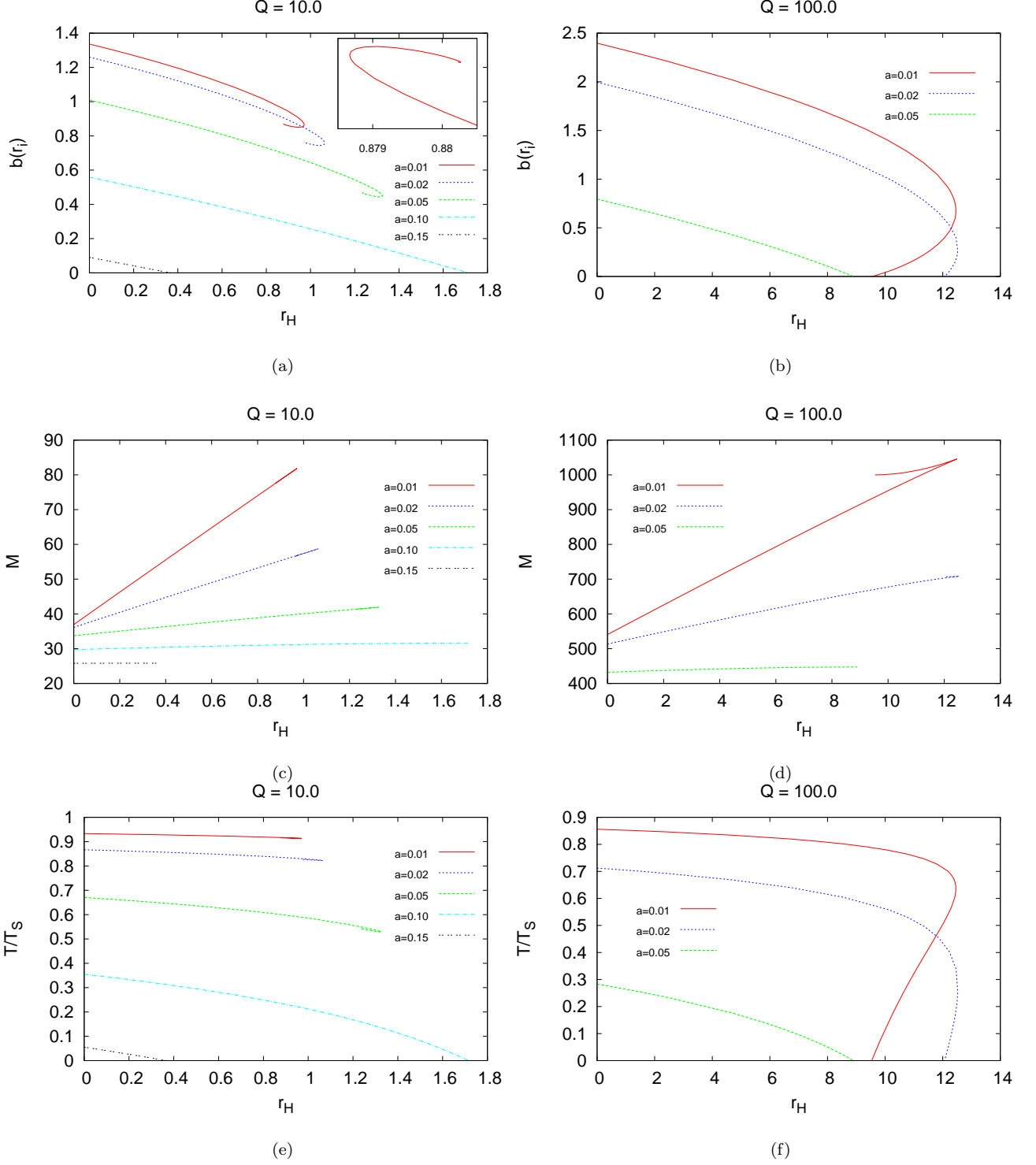


Figure 4: Properties of the black hole solutions with Schwarzschild-type interior shown versus the horizon radius r_H : The left column exhibits for solutions with fixed charge $Q = 10$ (a) $b(r_i)$, the value of the gauge field function $b(r)$ at the inner shell radius r_i ; (c) the mass M ; (e) the ratio of the temperature T at the black hole horizon r_H to the corresponding Schwarzschild black hole temperature T_S . The right column ((b), (d), (f)) exhibits the same for solutions with fixed charge $Q = 100$. Note that $a = \alpha^2$.

region $0 \leq r \leq r_i$ is then determined by the function $N(r) = 1 - (r_H/r)$ and a constant function $A(r)$. Thus the event horizon resides at $r_H < r_i$. But the presence of the Q -shell outside the event horizon, makes the properties of the black hole differ from those of a pure Schwarzschild black hole.

Since with the event horizon size a further variable appears, which is an important physical quantity, we discuss the black hole properties with respect to the horizon radius r_H in the following. The metric and matter field functions for black holes with charge $Q = 10$ at gravitational coupling $\alpha^2 = 0.1$ are exhibited in Fig. 2 for several values of the horizon radius r_H .

To illustrate the domain of existence of such black hole solutions, we again choose a sequence of values for the gravitational coupling constant, but we now keep the charge Q fixed, as we vary the horizon radius, starting from the corresponding globally regular Q -shell solution. A respective set of solutions is shown in Fig. 4 for $Q = 10$ and 100 .

First of all we note, that the horizon radius is always limited in size, where the maximal size grows with the charge Q . For small Q , e.g. $Q = 10$, we observe two distinct patterns for the black hole solutions. The first pattern arises when the fixed gravitational coupling constant has a value below a certain critical value. Here a maximal horizon size is reached, when the horizon radius r_H gets close to the inner radius of the shell r_i . There a bifurcation occurs and a second branch emerges, which ends at a second bifurcation, where a third branch emerges, etc. This results in a spiralling pattern, where the mass M and the temperature T of the solutions tend towards finite limiting values. (The first few branches are apparent in Fig. 4(a), and enlarged in the inset for a representative value of the gravitational coupling constant, $\alpha^2 = 0.01$, while the higher branches are too small to be resolved there.)

The second pattern is present above that critical value of the coupling constant. Here the set of black hole solutions for fixed gravitational coupling ends, when a throat is formed at the outer shell radius r_o . There the condition for extremal RN solutions, $r_o = \alpha^2 M = \alpha Q$, is satisfied again, as seen in Figs. 4(c) and 4(d). As the throat forms, the temperature T at the event horizon of the Schwarzschild-like black hole $r_H < r_i$ tends to zero, as seen in Figs. 4(e) and 4(f).

While appearing at first unexpected, the reason for the vanishing of the temperature T is the behaviour of the metric function $A(r)$ in g_{tt} , since $A(r)$ tends to zero in the interior, when the throat is formed, as seen in Fig. 2(a). We recall, that the ratio of the temperature T of the black hole within the Q -shell to the temperature $T_S = (4\pi r_H)^{-1}$ of the Schwarzschild black hole is given by $T/T_S = rAN'|_{r_H} = A(r_H)$.

For larger (fixed) values of the charge we always observe this second pattern, although the throat may either be reached directly after a monotonic increase of the horizon radius r_H to its maximum value, or along a second branch, where the horizon radius is decreasing again (having passed a bifurcation), as seen in Fig. 4(b).

As seen in the figure, whenever bifurcations occur, there are two (or more) black hole space-times with the same value of the charge Q and the same horizon radius r_H (within a certain range of values), but different values of the total mass M as measured at infinity. Surprisingly, however, there are also two (or more) black hole space-times with the same value of the charge Q and the same value of the total mass M (within a certain range of values). These black holes thus have the same set of global charges but are otherwise distinct solutions of the Einstein-matter equations. Consequently black hole uniqueness does not hold in this model of scalar electrodynamics.

Let us finally consider some mass relations for these black holes space-times possessing Q -shells. We begin by recalling an interesting result obtained in the isolated horizon framework [13]. It states that the mass M of a black hole space-time with horizon radius r_H and the mass M_{reg} of the corresponding globally regular space-time obtained in the limit $r_H \rightarrow 0$ are related via [14, 15, 13]

$$M = M_{\text{reg}} + M_{\Delta}, \quad (30)$$

where the mass contribution M_{Δ} is defined by

$$M_{\Delta} = \frac{1}{\alpha^2} \int_0^{r_H} \kappa(r'_H) r'_H dr'_H. \quad (31)$$

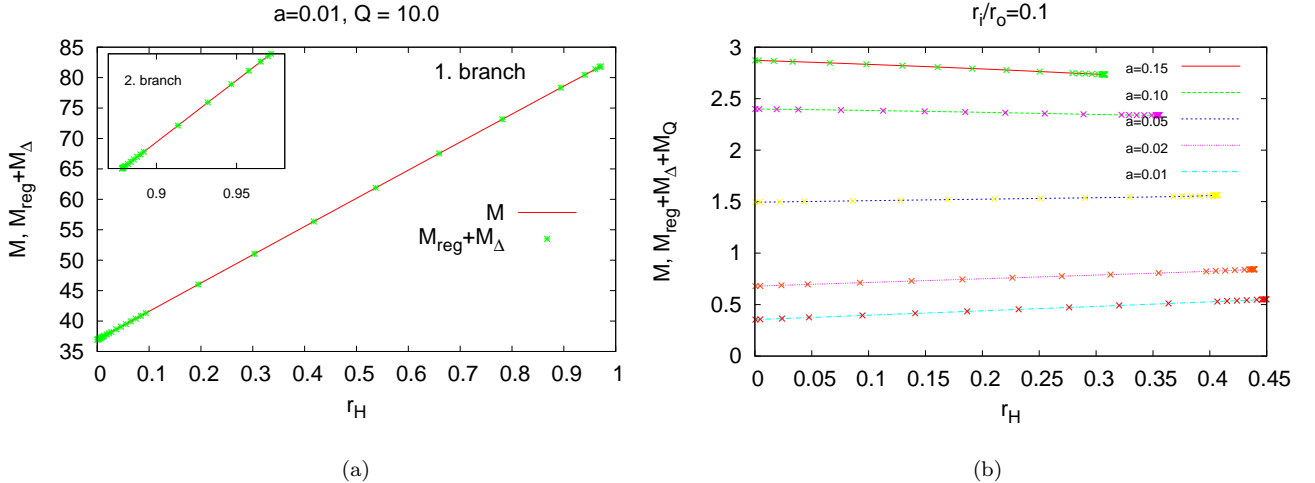


Figure 5: Mass formulae for black hole solutions: (a) the mass M of solutions with fixed charge $Q = 10$ and fixed gravitational coupling constant α , obtained from the asymptotic metric (26) and the mass formula (30); (b) the mass M of solutions with variable charge Q but fixed ratio of inner and outer shell radii r_i/r_o for several fixed values of the gravitational coupling constant α , obtained from the asymptotic metric (26) and the mass formula (33). Note that $a = \alpha^2$.

Here $\kappa(r_H)$ represents the surface gravity of the black hole with horizon radius r_H , $\kappa = 2\pi T$. Accordingly, the mass M of a space-time with a black hole with horizon radius r_H within a Q -shell with total charge Q should be obtained as the sum of the globally regular gravitating Q -shell with charge Q and the integral M_Δ along the set of black hole space-times, obtained by increasing the horizon radius for fixed charge from zero to r_H .

This relation is demonstrated in Fig. 5(a) for the set of solutions with charge $Q = 10$ and gravitational coupling constant $\alpha^2 = 0.01$. The values for the mass M obtained from the relation (31) are seen to agree with the values for the black hole mass M obtained from the asymptotics (26). The set of solutions exhibited has spiralling character, i.e., it has besides the main first branch a second branch, also exhibited, and further branches, not resolved in the figure.

When the charge is allowed to vary, too, one expects a change of the above relation in accordance with (28) and the first law (in the units employed), i.e.,

$$dM = \frac{\kappa}{8\pi\alpha^2} d\mathcal{A} + b(\infty)dQ, \quad (32)$$

where $\mathcal{A} = 4\pi r_H^2$ denotes the area of the horizon and $b(\infty)$ represents the electrostatic potential at infinity. Thus we generalize the above relation (30) to read

$$M = M_{\text{reg}} + M_\Delta + M_Q = M_{\text{reg}} + M_\Delta + \int_{Q_{\text{reg}}}^Q b(\infty)dQ'. \quad (33)$$

This relation is demonstrated in Fig. 5(b), where for several values of the gravitational coupling constant and for fixed ratio of inner and outer shell radii r_i/r_o , the values for the mass M obtained from the relation (33) are shown together with the values for the mass M obtained from the asymptotics (26).

6 Conclusion and Outlook

We have considered boson stars, gravitating Q -shells and black holes within Q -shells in scalar electrodynamics with a V -shaped scalar potential, where the scalar field is finite only in compact ball-like or shell-like regions.

The gravitating Q -shells surround a flat Minkowski-like interior region, while their exterior represents part of an exterior RN space-time. When the flat interior is replaced by a Schwarzschild-like interior, black hole space-times result, where a Schwarzschild-like black hole is surrounded by a compact shell of charged matter, whose exterior again represents part of an exterior RN space-time.

These black hole space-times violate black hole uniqueness, in certain regions of parameter space. Here for the same values of the mass M and the charge Q two or more distinct solutions of the Einstein-matter equations exist.

The solutions satisfy certain relations of the type obtained first in the isolated horizon formalism, which connect the mass M of a black hole solution with the mass M_{reg} of the associated globally regular solution. The masses of two regular solutions are related in an analogous (simpler) manner. This formalism further suggests to interpret the black hole space-times as bound states of Schwarzschild-type black holes and gravitating Q -shells [15].

While we have restricted our discussion here to Schwarzschild-type black holes in the interior, there are also black hole space-times with charged, i.e., Reissner-Nordström-type interior solutions. These more general black hole space-times will be discussed elsewhere.

The inclusion of rotation presents another interesting generalization of the solution considered here, since rotating boson stars are well-known [7, 8, 16, 17, 18]. The construction of the corresponding rotating shells and their black hole generalizations, however, still poses a challenge.

Acknowledgement

BK gratefully acknowledges support by the DFG, CL and ML by the DLR.

References

- [1] R. Friedberg, T. D. Lee and A. Sirlin, *Phys. Rev. D* **13**, 2739 (1976).
- [2] S. R. Coleman, *Nucl. Phys. B* **262**, 263 (1985) [Erratum-ibid. B **269**, 744 (1986)].
- [3] H. Arodz and J. Lis, *Phys. Rev. D* **77**, 107702 (2008) [arXiv:0803.1566 [hep-th]].
- [4] H. Arodz and J. Lis, arXiv:0812.3284 [hep-th].
- [5] T. D. Lee and Y. Pang, *Phys. Rept.* **221**, 251 (1992).
- [6] P. Jetzer, *Phys. Rept.* **220**, 163 (1992).
- [7] E. W. Mielke and F. E. Schunck, *Nucl. Phys. B* **564**, 185 (2000) [arXiv:gr-qc/0001061].
- [8] F. E. Schunck and E. W. Mielke, *Class. Quant. Grav.* **20**, R301 (2003) [arXiv:0801.0307 [astro-ph]].
- [9] J. D. Bekenstein, *Phys. Rev. D* **5**, 1239 (1972).
- [10] J. D. Bekenstein, *Phys. Rev. D* **51**, 6608 (1995).
- [11] A. E. Mayo and J. D. Bekenstein, *Phys. Rev. D* **54**, 5059 (1996) [arXiv:gr-qc/9602057].
- [12] R. M. Wald, *General Relativity* (University of Chicago Press, Chicago, 1984)
- [13] A. Ashtekar and B. Krishnan, *Living Rev. Rel.* **7**, 10 (2004) [arXiv:gr-qc/0407042].
- [14] A. Corichi and D. Sudarsky, *Phys. Rev. D* **61**, 101501 (2000) [arXiv:gr-qc/9912032].
- [15] A. Ashtekar, A. Corichi and D. Sudarsky, *Class. Quant. Grav.* **18**, 919 (2001) [arXiv:gr-qc/0011081].
- [16] S. Yoshida and Y. Eriguchi, *Phys. Rev. D* **56**, 762 (1997).

- [17] B. Kleihaus, J. Kunz and M. List, Phys. Rev. D **72**, 064002 (2005) [arXiv:gr-qc/0505143].
- [18] B. Kleihaus, J. Kunz, M. List and I. Schaffer, Phys. Rev. D **77**, 064025 (2008) [arXiv:0712.3742 [gr-qc]].